This is the accepted manuscript made available via CHORUS. The article has been published as:

WIMPless dark matter in anomaly-mediated supersymmetry breaking with hidden QED

Jonathan L. Feng, Vikram Rentala, and Ze'ev Surujon

Phys. Rev. D **84**, 095033 — Published 28 November 2011

DOI: 10.1103/PhysRevD.84.095033

UCI-TR-2011-16

WIMPless Dark Matter in Anomaly-Mediated Supersymmetry Breaking with Hidden QED

Jonathan L. Feng,[1] Vikram Rentala,[2,1] and Ze'ev Surujon[1,3]

[1]*Department of Physics and Astronomy, University of California, Irvine, CA 92697, USA*

[2]*Department of Physics, University of Arizona, Tucson, AZ 85721, USA*

[3]*Department of Physics and Astronomy, University of California, Riverside, CA 92521, USA*

Abstract

In anomaly-mediated supersymmetry breaking, superpartners in a hidden sector have masses that are proportional to couplings squared, and so naturally freeze out with the desired dark matter relic density for a large range of masses. We present an extremely simple realization of this possibility, with WIMPless dark matter arising from a hidden sector that is supersymmetric QED with N_F flavors. Dark matter is multi-component, composed of hidden leptons and sleptons with masses anywhere from 10 GeV to 10 TeV, and hidden photons provide the thermal bath. The dark matter self-interacts through hidden sector Coulomb scatterings that are potentially observable. In addition, the hidden photon contribution to the number of relativistic degrees of freedom is in the range $\Delta N_{\rm eff} \sim 0 - 2$, and, if the hidden and visible sectors were initially in thermal contact, the model predicts $\Delta N_{\rm eff} \sim 0.2 - 0.4$. Data already taken by Planck may provide evidence of such deviations.

PACS numbers: 95.35.+d, 12.60.Jv

I. INTRODUCTION

The thermal relic density of a particle X has the parametric dependence

$$\Omega_X \propto \frac{1}{\langle \sigma_{\rm an} v \rangle} \sim \frac{m_X^2}{g_X^4} \ , \tag{1}$$

where $\langle \sigma_{\rm an} v \rangle$ is the thermally-averaged product of the annihilation cross section and relative velocity, and m_X and g_X are the characteristic mass scale and coupling determining this cross section. The "WIMP miracle" is the fact that, for particles with weak scale masses and interactions, $g_X \sim g_{\rm weak} \sim 0.6$ and $m_X \sim m_{\rm weak} \sim 100$ GeV $-$ 1 TeV, the resulting thermal relic density is $\Omega_X \sim 0.1$, as desired for dark matter. This coincidence is the primary linchpin connecting the high energy and cosmic frontiers, and it has driven much of the research, both theoretical and experimental, in dark matter for decades.

At the same time, as Eq. (1) makes clear, the required thermal relic density may be realized by lighter and more weakly interacting particles (or heavier and more strongly interacting particles), provided their masses and couplings scale together to leave Ω_X invariant. Remarkably, particles with exactly these properties are found in supersymmetric theories that are motivated not by cosmology, but by particle physics [1, 2]. This fact, the "WIMPless miracle," suggests that, at least in the context of supersymmetry, the requirement of a correct thermal relic density does not necessarily lead to WIMPs and all of their accompanying phenomena, but rather argues for a more general viewpoint with a broader set of implications for both experiments and astrophysical observations [3–14].

In this work, we consider supersymmetric models with anomaly-mediated supersymmetry breaking (AMSB) [15, 16] and a hidden sector, that is, a set of particles with no standard model gauge interactions. In AMSB, the standard model is sequestered from the supersymmetry-breaking sector, for example, by being located on a different brane in extra dimensions [15], or because the supersymmetry-breaking sector is near-conformal over some energy range [17]. This sequestering implies that new physics contributions to flavor- and CP-violating observables are suppressed, which is the prime phenomenological virtue of AMSB.[1] We assume that the hidden sector is also sequestered. The superpartner masses in

[1] Both left- and right-handed sleptons are tachyonic in the minimal realization of AMSB. Our main concern here will be model-building in the hidden sector, and we assume that this visible sector problem is resolved by one of the many proposed mechanisms; see, for example, Refs. [18–20].

both the visible and hidden sectors then have the form

$$\tilde{m} \sim \frac{g^2}{16\pi^2} M_{3/2} \ , \tag{2}$$

where g represents the superpartner's interaction couplings and $M_{3/2} \sim 100$ TeV is the gravitino mass. Superpartners X in the hidden sector therefore satisfy

$$\frac{m_X}{g_X^2} \sim \frac{1}{16\pi^2} M_{3/2} \sim \frac{m_{\rm weak}}{g_{\rm weak}^2} \ , \tag{3}$$

where m_X and g_X are the hidden superpartner's mass and gauge coupling, and so realize the WIMPless miracle.

Although Eq. (3) goes a long way toward providing an attractive dark matter scenario, it is, of course, not sufficient. To realize the WIMPless scenario fully, the dark matter candidate must also (1) be stable on cosmological time scales and (2) annihilate to light particles, *i.e.*, the thermal bath, with cross section $\sigma_{\rm an} \sim g_X^4/m_X^2$. In addition, the model must also satisfy basic constraints, such as vacuum stability and perturbativity, and the dark matter's properties must be consistent with all experimental and observational constraints. These are not trivial constraints in the context of AMSB models, in which all superpartner masses are determined by a small number of low-energy parameters. Of course, this property also makes the scenarios more predictive, a highly laudable feature given the usual standards of hidden sector scenarios.

The possibility of WIMPless dark matter in AMSB was previously considered in Ref. [21]. There, non-Abelian gauge interactions in the hidden sector were considered, and a number of viable models were constructed. Here we consider hidden sectors with Abelian gauge interactions. We find that a simple scenario with hidden supersymmetric QED (SQED) satisfies all constraints, and at the same time predicts new phenomena that may be tested by near future astrophysical observations.

II. SQED IN AMSB

A. First Pass: $N_F = 1$

We consider SQED in the hidden sector, a U(1) gauge interaction with gauge coupling g. For pure SQED in AMSB, the photino is massless and interaction-less, and there is no

cold dark matter candidate. We therefore begin by introducing one flavor of matter, that is, a pair of superfields $\hat{e}_+$ and $\hat{e}_-$ with charges $+1$ and -1, respectively, which contain component fermions (electrons) $e_\pm$ and scalars (selectrons) $\tilde{e}_\pm$.

The AMSB soft masses are well-known [15, 16], and the relevant formulae are summarized in the first Appendix of Ref. [21]. For this simple model, the soft contributions to the photino mass and selectron masses are

$$m_{\tilde{\gamma}} = b\frac{g^2}{16\pi^2}M_{3/2} \tag{4}$$

$$m^2_{\tilde{e}_\pm} = -2b\left[\frac{g^2}{16\pi^2}M_{3/2}\right]^2 , \tag{5}$$

where $b = 2$ is the one-loop β-function coefficient. All A-terms vanish, since there are no Yukawa couplings. Because the gauge interaction is not asymptotically-free ($b > 0$), the selectrons are tachyonic. This is the source of the well-known tachyonic slepton problem in the visible sector of minimal AMSB models. The potential is therefore unstable in the D-flat direction $\langle\tilde{e}_+\rangle = \langle\tilde{e}_-\rangle$. Supergravity interactions could stabilize the potential, but generically, one would then expect the scalars to acquire Planck-scale vacuum expectation values, which is incompatible with the possibility of a WIMPless dark matter candidate.

To stabilize the potential, we may introduce a mass term in the superpotential $W = \mu\hat{e}_+\hat{e}_-$. We do not specify the source of this mass term; presumably it is generated by a mechanism similar to one that generates the μ-term in the visible sector. For now we assume there is a mechanism to generate a mass $\mu \sim (g^2/16\pi^2)M_{3/2}$, and analyze the phenomenological implications with μ as a free parameter. We return to this discussion in Sec. VI when the phenomenologically-allowed regions of parameter space have been established.

As an illustration of the utility of this approach, we note that with this mass term, the physical masses of the particles are

$$m_{\tilde{\gamma}} = b\frac{g^2}{16\pi^2}M_{3/2} \tag{6}$$

$$m_e = |\mu| \tag{7}$$

$$m_{\tilde{e}_\pm} = \left[|\mu|^2 - 2b\left(\frac{g^2}{16\pi^2}M_{3/2}\right)^2\right]^{1/2} \tag{8}$$

$$m_\gamma = 0 \ . \tag{9}$$

Vacuum stability requires that the selectrons be non-tachyonic. As a result, U(1) and R-parity are conserved. Photons are massless and form the thermal bath, selectrons are

stable by U(1) charge conservation, and electrons are stable by U(1) charge and R-parity conservation.

Unfortunately, vacuum stability also implies $m_e > m_{\tilde{\gamma}}$. The decay $\tilde{\gamma} \to \tilde{e}e$ is therefore forbidden, and photinos are also stable. This is problematic: photinos annihilate through $\tilde{\gamma}\tilde{\gamma} \to \gamma\gamma$, which is loop-suppressed, with cross section $\sigma_{\rm an} \sim (g^2/16\pi^2)^2 g^4/m_{\tilde{\gamma}}^2$, and so the photino is overproduced. This problem persists even if a soft supersymmetry-breaking B-term is introduced. Thus, for all values of μ, irrespective of how it is generated, we see that this scenario cannot provide a viable WIMPless dark matter model.

B. Viable Models: $N_F \geq 2$

We may build a viable model, however, by introducing additional charged matter fields to raise the photino mass and allow it to decay. In general, consider N_F pairs of superfields $\hat{e}_{i+}$ and $\hat{e}_{i-}$, containing component field fermions (leptons) $e_{i\pm}$ and scalars (sleptons) $\tilde{e}_{i\pm}$, $i = 1, \ldots, N_F$, with charges $\pm q_i$, supersymmetric masses μ_i, and bilinear scalar couplings $B_i \tilde{e}_{i+}\tilde{e}_{i-}$. The superpotential is

$$W = \sum_{i=1}^{N_F} \mu_i \hat{e}_{i+}\hat{e}_{i-} \ , \tag{10}$$

and the physical masses of the particles in the theory are

$$m_{\tilde{\gamma}} = b\frac{g^2}{16\pi^2} M_{3/2} \tag{11}$$

$$m_{e_i} = |\mu_i| \tag{12}$$

$$m_{\tilde{e}_{i\,1,2}} = \left[|\mu_i|^2 - 2bq_i^2 \left(\frac{g^2}{16\pi^2} M_{3/2} \right)^2 \pm B_i \right]^{1/2} \tag{13}$$

$$m_\gamma = 0 \ , \tag{14}$$

where $b = 2\sum q_i^2$. This model has several symmetries: the U(1) gauge symmetry of SQED, a global $\mathrm{U}(1)^{N_F}$ lepton flavor symmetry (with its diagonal U(1) being the gauge symmetry), and R-parity, under which the photon and leptons are even whereas the photino and sleptons are odd. As a result of these symmetries, the N_F flavors of leptons and N_F flavors of sleptons are all stable, naturally yielding multi-component dark matter with the total relic density roughly evenly divided between each of the components.

For simplicity, consider a version of the general model with $q_i = 1$, $\mu_i = \mu$, and $B_i = 0$ for all i. The lepton flavor symmetry is enhanced to $\mathrm{SU}(N_F)$. Relaxing the assumption of

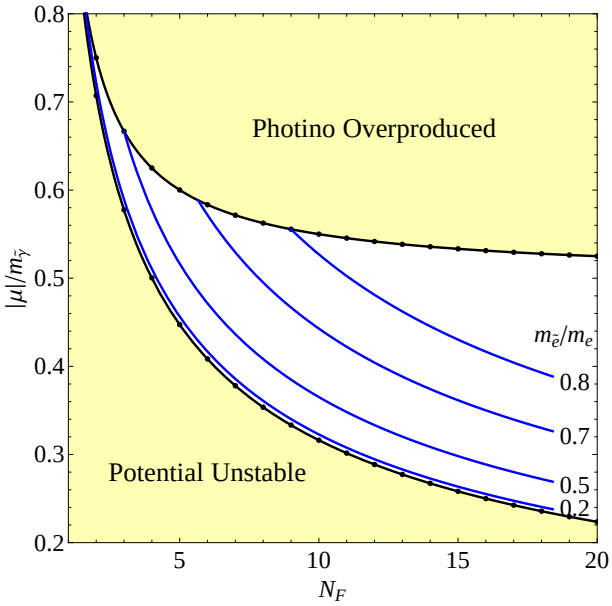

FIG. 1: Allowed region in the $(N_F, |\mu|/m_{\tilde{\gamma}})$ parameter space of WIMPless dark matter from hidden SQED with N_F flavors and global SU(N_F) flavor symmetry. The lower and upper shaded regions are excluded by the requirements that the vacuum be stable and photinos decay, respectively. In the allowed region, multi-component dark matter is composed of N_F degenerate flavors of hidden leptons e_i and N_F degenerate flavors of sleptons $\tilde{e}_i$. Contours of constant $m_{\tilde{e}_i}/m_{e_i}$ are shown.

universal masses and charges does not change our main conclusions qualitatively. As a very rough acknowledgment of this more general possibility, we present results for a continuous range of N_F, where non-integer N_F may capture some of the features of these less minimal scenarios. We also assume negligible mixing between the visible and hidden photons, as would be the case if the visible and hidden sectors are sequestered from each other, just as they are sequestered from the supersymmetry-breaking sector. We briefly mention the consequences of interactions between the two sectors via connectors in Sec. VI.

The resulting β-function coefficient is $b = 2N_F$, and the physical masses are

$$m_{\tilde{\gamma}} = 2N_F \frac{g^2}{16\pi^2} M_{3/2} \tag{15}$$

$$m_{e_i} = |\mu| \tag{16}$$

$$m_{\tilde{e}_{i\pm}} = \sqrt{|\mu|^2 - \frac{m_{\tilde{\gamma}}^2}{N_F}} \tag{17}$$

$$m_\gamma = 0\ . \tag{18}$$

The requirements of vacuum stability and photino instability constrain $|\mu|/m_{\tilde{\gamma}}$ from below

and above, respectively. The resulting allowed range

$$\frac{1}{\sqrt{N_F}} < \frac{|\mu|}{m_{\tilde{\gamma}}} < \frac{1}{2} + \frac{1}{2N_F} \ , \tag{19}$$

is shown in Fig. 1. As expected, there is no allowed range for $N_F = 1$, but for $N_F = 2$, there are viable models with

$$0.71 \lesssim \frac{|\mu|}{m_{\tilde{\gamma}}} < 0.75 \ , \tag{20}$$

and the allowed range expands as N_F increases. Non-zero B-terms would move both the lower and upper boundaries to larger values of $|\mu|/m_{\tilde{\gamma}}$. In the allowed region, $m_{\tilde{e}_i}$ and m_{e_i} are of the same order of magnitude in almost all of the parameter space, with $m_{\tilde{e}_i} \ll m_{e_i}$ only in a thin skin layer near the vacuum instability boundary, where $m_{\tilde{e}_i}$ vanishes.

III. RELIC DENSITY

The freeze out of hidden leptons and sleptons may be analyzed in the usual way, with the slight complication that the hidden sector may be at a different temperature than the visible sector. This possibility has been analyzed in detail [2, 22], and the results are summarized in the second Appendix of Ref. [21]. For a particle X that annihilates through S-wave processes with annihilation cross section

$$\sigma_{\rm an} v \approx \sigma_0 \equiv k_X \frac{\pi \alpha_X^2}{m_X^2} \ , \tag{21}$$

where k_X is an $\mathcal{O}(1)$ constant determined by the specific annihilation processes, the thermal relic density is

$$\Omega_X \approx \xi_f \, \frac{0.17 \text{ pb}}{\sigma_0} \simeq 0.23 \, \xi_f \, \frac{1}{k_X} \left[\frac{0.025}{\alpha_X} \frac{m_X}{\text{TeV}} \right]^2 \ , \tag{22}$$

where $\xi_f \equiv T_f^{\rm h}/T_f^{\rm v}$ is the ratio of the hidden to visible sector temperatures when the hidden dark matter freezes out.

In the present case, both hidden leptons and sleptons annihilate to hidden photons through S-wave processes, and so the results above apply. Lepton pair annihilation $e_i \bar{e}_i \to \gamma\gamma$ is mediated by diagrams with leptons in the t- and u-channel, as in standard QED. Slepton pair annihilation $\tilde{e}_{i\pm} \tilde{e}^*_{i\pm} \to \gamma\gamma$ is mediated by similar diagrams with sleptons in the t- and u-channel, and also through four-point interactions. The annihilation coefficients are $k_{e_i} = 1$

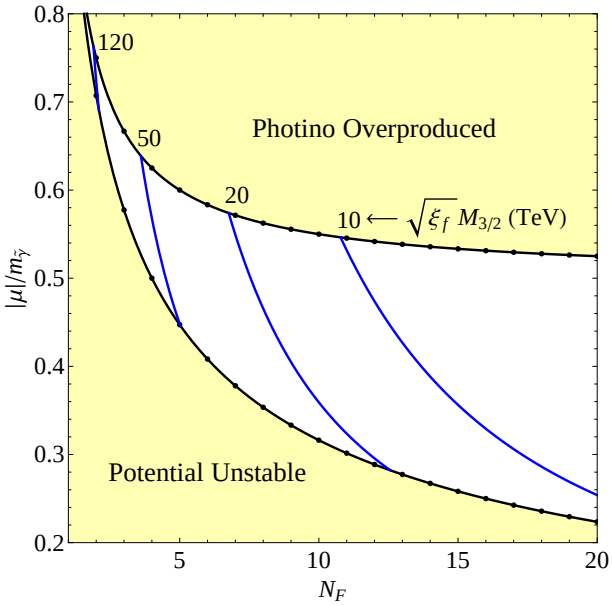

FIG. 2: Contours of constant $\sqrt{\xi_f} M_{3/2}$, as determined by requiring $\Omega_{\rm tot} \simeq 0.23$ in the $(N_F, |\mu|/m_{\tilde{\gamma}})$ parameter space.

and $k_{\tilde{e}_i} = 2$ [2, 23]. The resulting total relic density is therefore

$$\Omega_{\rm tot} \simeq 0.23\, \xi_f\, N_F \left[\frac{1}{k_{e_i}} \left(\frac{0.025}{\alpha} \frac{m_{e_i}}{\rm TeV} \right)^2 + \frac{2}{k_{\tilde{e}_i}} \left(\frac{0.025}{\alpha} \frac{m_{\tilde{e}_i}}{\rm TeV} \right)^2 \right] \tag{23}$$

$$= 0.23\, \frac{N_F^3}{6.3} \left(2\frac{|\mu|^2}{m_{\tilde{\gamma}}^2} - \frac{1}{N_F} \right) \left(\frac{\sqrt{\xi_f}\, M_{3/2}}{100\ {\rm TeV}} \right)^2 , \tag{24}$$

where, in the second line, we have substituted the appropriate values of $k_{e_i,\tilde{e}_i}$ and $m_{e_i,\tilde{e}_i}$. As required for a realization of the WIMPless miracle, the relic density is independent of the gauge coupling, provided $|\mu| \sim m_{\tilde{\gamma}}$, as discussed above.

In Fig. 2, we set $\Omega_{\rm tot} \simeq 0.23$ and plot contours of constant $\sqrt{\xi_f} M_{3/2}$ in the $(N_F, |\mu|/m_{\tilde{\gamma}})$ plane. LEP2 constraints require Wino masses $m_{\tilde{W}} > 92 - 103$ GeV, depending on the chargino-neutralino mass difference [24]. Assuming the minimal AMSB relation for the Wino mass, this implies $M_{3/2} \simeq 372\, m_{\tilde{W}} \gtrsim 34$ TeV. The LHC also bounds the AMSB scenario, but these constraints depend on the spectrum of strongly-interacting superpartners. As a conservative example, current bounds from the LHC require $m_{\tilde{g}} \gtrsim 800$ GeV for large squark masses [25], which implies $M_{3/2} \simeq 35\, m_{\tilde{g}} \gtrsim 28$ TeV. These LHC bounds will certainly improve rapidly. At the moment, however, the LEP2 bounds may serve as a guide to what is allowed, and we consider $M_{3/2} \approx 34$ TeV to be the lower bound, and values of $M_{3/2}$ just above 34 TeV to be the most natural from the point of the gauge hierarchy problem. For ξ_f,

perhaps the most motivated values are $\xi_f \sim 1$, as would result, for example, if the hidden and visible sectors were similarly reheated through inflaton decay [26, 27], or, as discussed below, if they were in thermal contact in the very early Universe. For these values of $M_{3/2}$ and ξ_f, we see from Fig. 2 that the hidden leptons and sleptons are excellent cold dark matter candidates, independent of their mass (or equivalently, the gauge coupling).

For comparison, note that the visible sector's Wino may also be cold dark matter. However, given that SU(2) is "accidentally" nearly conformal in the minimal supersymmetric standard model (MSSM), AMSB Winos annihilate very efficiently and have the correct thermal relic density only for very large masses $m_{\tilde{W}} \sim 3$ TeV [16]. In minimal models, this implies $m_{\tilde{g}} \sim 30$ TeV and $M_{3/2} \sim 1100$ TeV, highly unnatural values if AMSB supersymmetry is to be a solution to the gauge hierarchy problem. The hidden sector scenario analyzed here rectifies this situation, in the sense that for the natural range $M_{3/2} \sim 100$ TeV where the relic abundance of visible sector superpartners is generically too low to contribute significantly to dark matter, the hidden leptons and sleptons have the desired abundances to be dark matter.

Finally, perhaps the most motivated possibility for relating the visible and hidden sector temperatures is to assume that these sectors were in thermal contact at very early times, but then decoupled. In this case, the ratio of temperatures at very early times is $\xi_\infty = 1$, where the subscript "∞" denotes the period of thermal coupling, and the ratio of temperatures at later times is determined by the visible and hidden sector particle spectra, assuming that after decoupling the entropy of each sector is separately conserved.

In particular, the ratio of temperatures at freeze out is related to ξ_∞ by

$$\xi_f = \left[\frac{g_*^{\rm h}(T_\infty^{\rm h})}{g_*^{\rm h}(T_f^{\rm h})} \, \frac{g_*^{\rm v}(T_f^{\rm v})}{g_*^{\rm v}(T_\infty^{\rm v})} \right]^{\frac{1}{3}} \xi_\infty \ , \tag{25}$$

where $g_*(T)$ is the number of relativistic degrees of freedom at temperature T. This depends on the presence or absence of very heavy degrees of freedom in the visible and hidden sectors. However, assuming a desert in the MSSM and our hidden SQED sectors, that is, no particles with masses between the temperature at which the two sectors thermally decoupled and the masses of the heaviest particles we have considered, $g_*^{\rm v}(T_\infty^{\rm v}) = g_*^{\rm MSSM} = 228.75$, the total number of degrees of freedom in the MSSM, and $g_*^{\rm h}(T_\infty^{\rm h}) = 7.5 N_F + 4$. At freeze out, we may take $g_*^{\rm h}(T_f^{\rm h}) = 2$, since the temperature at freeze out $T_f^{\rm h} \sim m_X/25$ is generically below all dark matter masses. In the visible sector, possible benchmark values for $g_*^{\rm v}(T_f^{\rm v})$ are 86.25, its

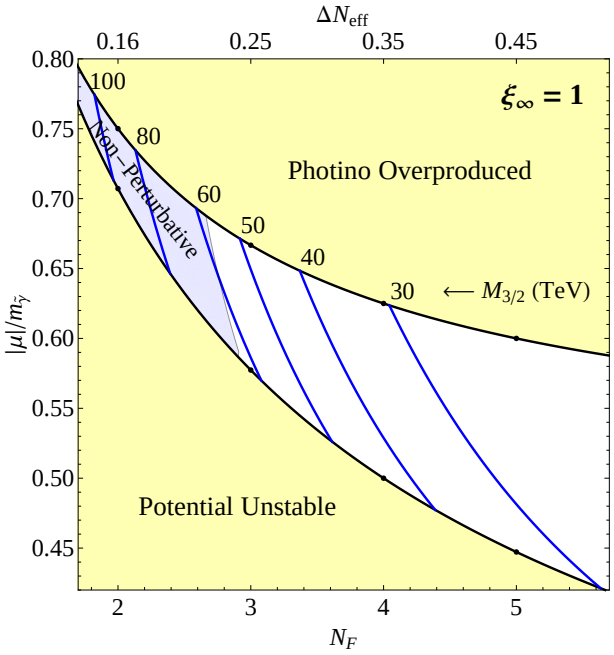

FIG. 3: Contours of constant $M_{3/2}$ in the $(N_F, |\mu|/m_{\tilde{\gamma}})$ plane, with fixed $\xi_\infty = 1$, $\Omega_{\rm tot} \simeq 0.23$, and $g_*^{\rm v}(T_f^{\rm v}) = g_*^{\rm SM}$. $\Delta N_{\rm eff}$ is the effective number of extra neutrinos, as given by Eq. (34). The shaded region labeled "Non-Perturbative" is forbidden by the considerations of self-interactions and perturbativity discussed in Sec. V. For fixed ξ_∞ and $\Omega_{\rm tot}$, $M_{3/2} \propto g_*^{\rm v}(T_f^{\rm v})^{-1/6}$.

SM value for temperatures between m_b and m_W, $g_*^{\rm SM} = 106.75$, the total g_* for the standard model, and $g_*^{\rm MSSM} = 228.75$. Normalizing to $g_*^{\rm v}(T_f^{\rm v}) = g_*^{\rm SM}$, we find

$$\xi_f = 1.21 \left[\left(N_F + \frac{8}{15} \right) \left(\frac{g_*^{\rm v}(T_f^{\rm v})}{106.75} \right) \right]^{\frac{1}{3}} \xi_\infty \ . \tag{26}$$

The ratio of temperatures ξ typically grows between very early times and freeze out, because almost the entire hidden sector becomes non-relativistic before freeze out, while this is not true for the visible sector.

In Fig. 3, we assume $\xi_\infty = 1$, and use Eq. (26) to determine ξ_f. Requiring $\Omega_{\rm tot} \simeq 0.23$ fixes $M_{3/2}$, and we present contours of constant $M_{3/2}$ in the $(N_F, |\mu|/m_{\tilde{\gamma}})$ plane. For large N_F, $M_{3/2}$ becomes small, and requiring $M_{3/2} \gtrsim 34$ TeV, its lower bound in minimal AMSB, implies $N_F \lesssim 5$.

These conclusions require significant assumptions, namely, that the visible and hidden sectors were initially in thermal contact and then decoupled, and that there is a desert. It is significant, though, that even with these restrictive assumptions, there is a viable parameter space with the correct dark matter relic density. In addition, as we will see in the next

section, this simple scenario is especially interesting, as it restricts the parameter space to regions of low N_F where the hidden sector may contribute significantly to extra relativistic degrees of freedom, a prediction that will be tested in the near future.

IV. CONTRIBUTIONS TO THE NUMBER OF RELATIVISTIC DEGREES OF FREEDOM

The massless photons of the hidden sector contribute to the number of relativistic degrees of freedom at any temperature. Their existence is therefore bounded by the standard theory of big bang nucleosynthesis (BBN) and observations of the cosmic microwave background (CMB), with testable consequences for future observations.

Constraints on the number of relativistic degrees of freedom are typically reported as constraints on the effective number of extra neutrinos

$$\Delta N_{\rm eff} \equiv N_{\rm eff} - N_{\rm eff}^{\rm SM} \ , \tag{27}$$

where $N_{\rm eff}^{\rm SM} \simeq 3.046$ deviates from 3 slightly because the three neutrinos of the standard model are not completely decoupled at the time of e^+e^- annihilation [28]. Current bounds are

$$\Delta N_{\rm eff} \ = \ 0.19 \pm 1.2 \ (95\% \ {\rm CL}) \ {\rm BBN} \tag{28}$$

$$\Delta N_{\rm eff} \ = \ 1.29^{+0.86}_{-0.88} \ (68\% \ {\rm CL}) \ {\rm CMB} \ , \tag{29}$$

where the BBN constraint assumes a baryon density that has been fixed to the value determined by the CMB, and both ^{4}He and D data are included [29, 30], and the CMB constraint is the WMAP 7-year result [31] that combines CMB observations with distance information from baryon acoustic oscillations, supernovae (SNIa) and Hubble constant measurements. The BBN and CMB results should be consistent, provided the number of relativistic degrees of freedom remains constant between visible sector temperatures of $T_{\rm BBN} \sim$ MeV and $T_{\rm CMB} \sim$ eV. The BBN result is fully consistent with the standard model, while the CMB result shows a 1.5σ excess. In the near future, Planck is expected to determine $N_{\rm eff}$ with a standard deviation of $\sigma(N_{\rm eff}) \approx 0.3$ [32–35], given only ~ 1 year of data. This will, of course, be improved with more data, and a future LSST-like survey may determine $N_{\rm eff}$ with a standard deviation of $\sigma(N_{\rm eff}) \approx 0.1$ [35]. Needless to say, if the current WMAP central value

remains and the uncertainty shrinks as expected, these measurements will have far-reaching consequences.

In hidden sector scenarios, $\Delta N_{\rm eff}$ is related to the number of light hidden degrees of freedom by

$$\Delta N_{\rm eff}\ \frac{7}{8}\ 2\ T_\nu^4 = g_*^{\rm h}(T_{\rm CMB}^{\rm h}) T_{\rm CMB}^{\rm h\,4}\ , \tag{30}$$

where $T_\nu = (4/11)^{1/3} T_{\rm CMB}^{\rm v}$. The effective number of extra neutrinos is therefore

$$\Delta N_{\rm eff} \ = \ \frac{4}{7}\left(\frac{11}{4}\right)^{\frac{4}{3}} g_*^{\rm h}(T_{\rm CMB}^{\rm h})\, \xi_{\rm CMB}^4 \tag{31}$$

$$= \ \frac{4}{7}\left(\frac{11}{4}\right)^{\frac{4}{3}} g_*^{\rm h}(T_{\rm CMB}^{\rm h})\ \left[\frac{g_*^{\rm h}(T_f^{\rm h})}{g_*^{\rm h}(T_{\rm CMB}^{\rm h})}\frac{g_*^{\rm v}(T_{\rm CMB}^{\rm v})}{g_*^{\rm v}(T_f^{\rm v})}\right]^{\frac{4}{3}} \xi_f^4\ . \tag{32}$$

At the time of CMB decoupling, $g_*^{\rm v}(T_{\rm CMB}^{\rm v}) = g_*^{\rm h}(T_{\rm CMB}^{\rm h}) = 2$. At freeze out, as discussed in Sec. III, $g_*^{\rm h}(T_f^{\rm h}) = 2$, but $g_*^{\rm h}(T_f^{\rm v})$ is more model-dependent. Normalizing to $g_*^{\rm v}(T_f^{\rm v}) = g_*^{\rm SM}$, we find

$$\Delta N_{\rm eff} = \left(\frac{\xi_f}{2.60}\right)^4 \left[\frac{106.75}{g_*^{\rm v}(T_f^{\rm v})}\right]^{\frac{4}{3}}\ . \tag{33}$$

Contours of $\Delta N_{\rm eff}$ are plotted in Fig. 4 for $M_{3/2} = 70$ TeV and 80 TeV. Note that $\Delta N_{\rm eff}$ is highly sensitive to $M_{3/2}$; requiring a fixed $\Omega_{\rm tot}$, $\Delta N_{\rm eff} \propto M_{3/2}^{-8}$. For the simplest case of $N_F = 2$, however, we find that $N_{\rm eff}$ may have large deviations from the standard model, with values up to $\Delta N_{\rm eff} \sim 2$ possible. Much smaller values consistent with the standard model within experimental uncertainties are also possible, however.

Finally, we note that the effective number of extra neutrinos may also be expressed in terms of ξ_∞. Assuming a desert between temperatures at very early times and the mass scales of the MSSM and hidden SQED particles,

$$\Delta N_{\rm eff} = 0.20\left(\frac{N_F + \frac{8}{15}}{3}\right)^{\frac{4}{3}} \xi_\infty^4\ . \tag{34}$$

This formula establishes a definite relation between $\Delta N_{\rm eff}$ and N_F, once ξ_∞ has been fixed. Such a prediction for $\Delta N_{\rm eff}$ is independent of many aspects of the model, such as $g_*^{\rm v}(T_f^{\rm v})$. If a nonzero value for $\Delta N_{\rm eff}$ is established, it will provide a strong motivation for hidden sectors, and, in the current context, assuming $\xi_\infty = 1$, it may be used to determine N_F. Since fixing ξ_∞ also determines $M_{3/2}$ unambiguously for every point on the $(|\mu|/m_{\tilde\gamma}, N_F)$ plane, collider bounds on $M_{3/2}$ imply that $\Delta N_{\rm eff}$ is constrained too. From Fig. 3 we can see that $\Delta N_{\rm eff}$ must be below ~ 0.4 if indeed $\xi_\infty = 1$ and if the dark matter content of the

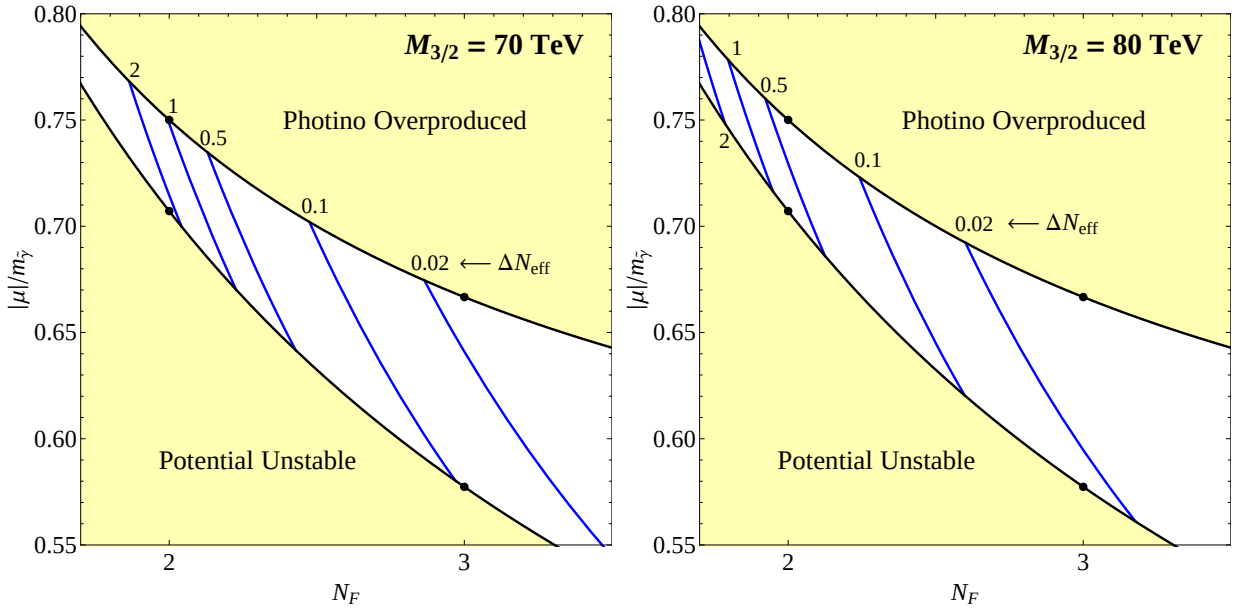

FIG. 4: Contours of constant $\Delta N_{\rm eff}$, the effective number of extra neutrinos in the $(N_F, |\mu|/m_{\tilde{\gamma}})$ parameter space for $M_{3/2} = 70$ and 80 TeV, $\Omega_{\rm tot} \simeq 0.23$, and $g_*^{\rm v}(T_f^{\rm v}) = g_*^{\rm SM}$. For fixed $\Omega_{\rm tot}$, $\Delta N_{\rm eff} \propto M_{3/2}^{-8}\, g_*^{\rm v}(T_f^{\rm v})^{-4/3}$.

Universe is to be explained by this model. In the next section we show that astrophysical constraints from self-interactions further limit the parameter space, placing a lower bound on $\Delta N_{\rm eff}$ of ~ 0.2, increasing the predictivity of $\Delta N_{\rm eff}$.

V. SELF-INTERACTIONS

In calculating the relic density, the dark matter's coupling α_X and mass m_X drop out. However, the hidden leptons and sleptons are self-interacting through Coulomb interactions, and the requirement that these self-interactions not violate observational bounds imposes constraints on α_X and m_X.

Dark matter self-interactions are constrained by several observations, and the case of long-range Coulomb interactions has been considered recently in Refs. [23, 36]. There are several possible constraints on charged hidden dark matter. For example, one might worry that the annihilation of charged particles could be enhanced by Sommerfeld enhancement or by bound state formation in either the early Universe or in protohalos. It turns out that the enhancement to the annihilation cross section from these effects is typically negligible, at least if the dark matter annihilates only to hidden sector particles. The most stringent

constraint is from the observation of elliptical halos; dark matter self-interactions cannot be so strong that the resulting energy transfer between dark matter particles would have caused these halos to relax to become spherical [23, 37].

Neglecting sub-dominant s-channel contributions to the energy transfer cross section, the relaxation time is [23]

$$\tau_{\rm r} \simeq \frac{m_X^3 v_0^3}{4\sqrt{\pi}\alpha_X^2 \rho_X C} \ , \tag{35}$$

where

$$C \approx \ln\left[\frac{\left(b_{\rm max} m_X v_0^2 \alpha_X^{-1}\right)^2 + 1}{2}\right] \tag{36}$$

is the Coulomb logarithm,

$$b_{\rm max} \sim \frac{m_X v_0}{\sqrt{4\pi\alpha_X \rho_X}} \tag{37}$$

is the Debye screening length, and v_0 and ρ_X are the velocity dispersion and mass density, respectively, of dark matter particles at a distance from the galactic center where the halo has been established to be elliptical. Following the analysis of Ref. [23], observations of the elliptical galaxy NGC 720 [38, 39] have established an elliptical halo at distances $r \sim 3 - 10$ kpc from the center, with mass density $\rho_X(r) = 3.5 - 0.7$ GeV/cm^3 and velocity $v_0 = 270 - 250$ km/s in this range of radii. Over this range, the estimate for $\tau_{\rm r}$ varies by a factor of 4. Taking the values of ρ_X and v_0 at $r \sim 3$ kpc, which yields the most stringent limit, we find

$$\tau_{\rm r} \simeq 9.0 \times 10^9 \ {\rm yr} \left(\frac{m_X}{\rm TeV}\right)^3 \left(\frac{0.01}{\alpha_X}\right)^2 \ \frac{90}{C} \ , \tag{38}$$

where C has been normalized to a typical value. We may derive bounds by requiring $\tau_{\rm r} > 10^{10}$ yr.

In our multi-component model of dark matter, the mass m_X in Eq. (38) is ambiguous. However, for nearly degenerate m_{e_i} and $m_{\tilde{e}_i}$, we may take either one, of course, and for highly non-degenerate cases, we may take the heavier mass m_{e_i}, since the thermal relic density scales as m_X^2, and so the relic density of the lighter species becomes insignificant. For simplicity, and given the other uncertainties of the analysis, we therefore identify the lepton mass as the representative mass and set $m_X = m_{e_i}$.

For fixed $M_{3/2}$ and a given point in the $(N_F, |\mu|/m_{\tilde{\gamma}})$ plane, $\alpha_X \propto m_{e_i}$. Substituting this relation in Eq. (38), requiring $\tau_{\rm r} > 10^{10}$ yr, and setting the Coulomb logarithm to be

$C = 90$, we find that the observation of elliptical halos implies the lower bound

$$m_{e_i} > m_{\rm DM}^{\rm min} \equiv \left[\frac{6.6}{N_F\,(\mu/m_{\tilde\gamma})}\right]^2 \left(\frac{100\ {\rm TeV}}{M_{3/2}}\right)^2 {\rm TeV}\ . \tag{39}$$

Equation (39) places a lower bound on the dark matter mass, but there is also an upper bound. Implicit in the formulae for the AMSB soft masses is the assumption that the hidden sector particles discussed are in fact present in the low-energy theory. This requires that all superpartner masses, in particular, the photino, be below $M_{3/2}$, implying

$$\frac{m_{\tilde\gamma}}{M_{3/2}} = 2N_F\frac{\alpha_X}{4\pi} < 1\ . \tag{40}$$

This same criterion may be taken as required to ensure perturbativity, that is, that the leading-order expressions for the soft supersymmetry-breaking masses are reliable.[2] Taking Eq. (40) as our perturbativity requirement, and again setting $C = 90$, implies

$$\frac{\mu}{m_{\tilde\gamma}} > \left(\frac{0.66}{N_F}\right)^{\frac{2}{3}} \frac{100\ {\rm TeV}}{M_{3/2}}\ . \tag{41}$$

If, for a certain region of parameter space, this upper bound on α_X conflicts with the lower bound on α_X from halo shapes, that region of parameter space is excluded.

Lower bounds on the dark matter mass and a region of non-perturbativity are shown in Fig. 5. From the $M_{3/2} = 40$ TeV panel, we see that the perturbativity constraint excludes otherwise viable regions in the parameter space with low N_F if $M_{3/2}$ is very low. We find, however, that it does not constrain the allowed parameter space with $N_F \geq 2$ if $M_{3/2} \gtrsim 65$ TeV. From the $M_{3/2} = 80$ TeV panel, we see that the regions with large $\Delta N_{\rm eff} \sim 1$ of Fig. 4 have heavy dark matter, with $m_{\rm DM}^{\rm min} \sim 8 - 30$ TeV.

Finally, from all the panels, we see that as N_F increases, $m_{\rm DM}^{\rm min}$ decreases. For a fixed $|\mu|/m_{\tilde\gamma}$, increasing N_F implies lower α_X, weakening the self-interaction constraint, and making lighter dark matter masses possible. From the $M_{3/2} = 200$ and 500 TeV panels, we see that dark matter masses as low as ~ 10 GeV are possible. For $M_{3/2} \sim 500$ TeV, light dark matter is allowed for $N_F \sim 30$ by all constraints. In contrast to WIMPs, which have masses typically in the range 100 GeV $-$ 1 TeV, this WIMPless scenario allows a much broader range of dark matter masses, while preserving the required relic density. The lower bound

[2] Note that the requirement that the gauge coupling does not reach its Landau pole below the gravitino mass, $\Lambda \sim m_{\tilde\gamma}{\rm exp}[2\pi/(b\alpha_X)] = m_{\tilde\gamma}{\rm exp}[M_{3/2}/(2m_{\tilde\gamma})] > M_{3/2}$, is always satisfied.

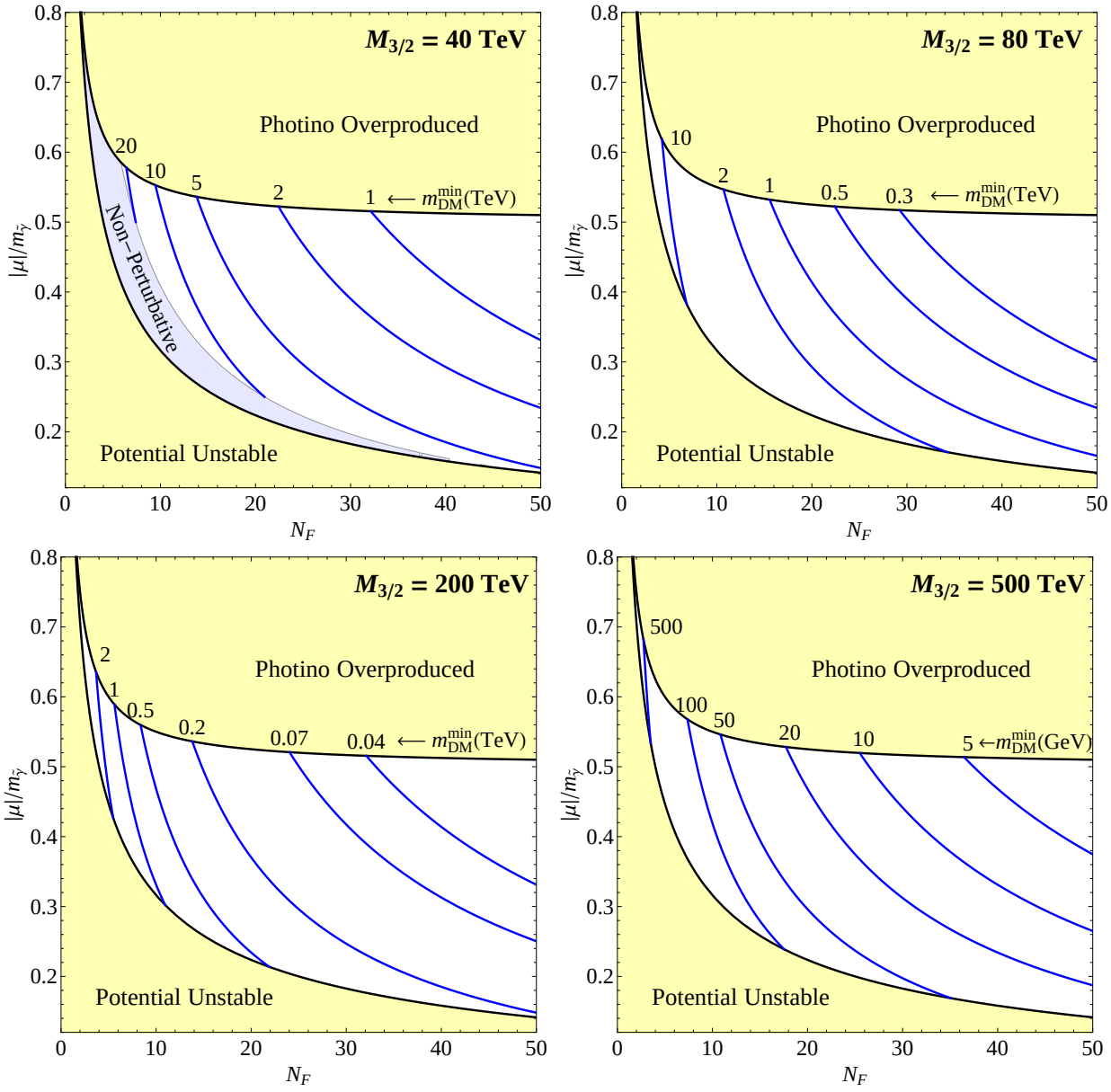

FIG. 5: Contours of constant $m_{\rm DM}^{\rm min}$, the minimal lepton mass that is consistent with self-interaction bounds from the observation of elliptical halos, for $M_{3/2} = 40, 80, 200$, and 500 TeV, and $\Omega_{\rm tot} = 0.23$. In the shaded region marked "Non-Perturbative," $m_{\tilde{\gamma}} > M_{3/2}$, signaling a breakdown of perturbativity. Note that the values of $m_{\rm DM}^{\rm min}$ are in units of GeV for the $M_{3/2} = 500$ TeV panel, and in TeV for the others, as indicated.

is imposed by the requirement that the self-interactions of charged dark matter not be too large, which is, of course, absent for WIMPs. Even so, the possibility of 10 GeV WIMPless dark matter remains, and is particularly interesting, given current hints of signals in this range from DAMA/LIBRA [40, 41] and CoGeNT [42, 43]. It would be interesting to in-

vestigate the possibility of adding connector fields charged under both visible sector gauge groups and the hidden U(1) to explain these signals.

At this point it is worth revisiting the discussion in Sec. IV regarding $\Delta N_{\rm eff}$. As mentioned before, once ξ_∞ is fixed, $M_{3/2}$ is determined for every point on the $(|\mu|/m_{\tilde{\gamma}}, N_F)$ plane. We may then use Eq. (41) to check whether such a point satisfies the requirement of perturbativity. The region excluded by this requirement is indicated in Fig. 3. From this we conclude that if $\xi_\infty = 1$, the model predicts that $\Delta N_{\rm eff}$ lies in the range $0.2 \sim 0.4$. Such a prediction will definitely be tested in the near future, as discussed in Sec. IV.

VI. DISCUSSION

In this work, we have constructed an extremely simple model of dark matter in AMSB with a hidden sector. The hidden sector is SQED with N_F degenerate flavors of leptons and sleptons. Through a combination of electric charge, lepton flavor, and R-parity conservation, all N_F flavors of leptons and sleptons are stable and contribute to cold dark matter. As in the case of WIMPs, the thermal relic density of these particles is directly related to the mechanism of electroweak symmetry breaking and is naturally of the right order of magnitude to be dark matter. In contrast to WIMPs, however, the dark matter has a mass that may be anywhere from ~ 10 GeV to 10 TeV, and it also has interesting astrophysical implications that are absent for WIMPs. In particular, it self-interacts through Coulomb interactions, and the massless hidden photon implies extra relativistic degrees of freedom in the range $\Delta N_{\rm eff} \sim 0 - 2$, with significant deviations from 0 possible in the simplest models with low $N_F = 2 - 5$. If the hidden and visible sectors were in thermal contact in the very early Universe, $\Delta N_{\rm eff}$ is more constrained and is predicted to assume values in the range $0.2 - 0.4$.

Our predictions for $\Delta N_{\rm eff}$ are especially interesting, given that data already taken by Planck may provide evidence of such deviations. Note that in the case where the hidden and visible sectors were in thermal contact, there is a fairly narrow prediction for $\Delta N_{\rm eff}$, which includes a lower bound. This is an interesting feature: generically, in hidden sectors there is enough model-building freedom to predict a large range of $\Delta N_{\rm eff}$, including values that are consistent with zero. In this WIMPless scenario, $\Delta N_{\rm eff}$ is connected to the number of flavors N_F through Eq. (26), and N_F is bounded by the relic density expression of Eq. (24),

since ξ_f is bounded by the assumption of thermal contact, and $M_{3/2}$ is bounded by its impact on the visible sector spectrum. The WIMPless scenario is therefore relatively constrained and predictive compared to generic hidden sector scenarios. Although the existence of extra relativistic degrees of freedom is a generic feature of hidden sectors, future indications for both $\Delta N_{\rm eff} > 0$ and self-interacting dark matter would highly motivate scenarios such as the one discussed here, and precise measurements could restrict proposed explanations further.

As dark matter in this model consists of hidden particles, the visible sector is relieved of the duty of providing dark matter. This is a welcome possibility, as the most natural dark matter candidate in AMSB, the neutral Wino, has a thermal relic density that is typically too small to be all of dark matter by several orders of magnitude. R-parity may also be broken in the visible sector, provided constraints from proton decay and elsewhere are not violated, removing the missing energy signals of supersymmetry, with strong implications for collider searches.

In this work, we have introduced μ, a supersymmetric mass for the hidden sleptons, and treated it as a free parameter. This is a time-honored approach and has yielded interesting results. That said, just as a complete neutralino WIMP scenario requires a solution to the μ problem in the visible sector, a complete WIMPless scenario requires a concrete μ-term mechanism in the hidden sector. Formally, to realize the WIMPless miracle with a relic density that is independent of g, the μ parameter must have the form $\mu \sim m_{\tilde{\gamma}} \sim (g^2/16\pi^2) M_{3/2}$. Of course, we have found that constraints from dark matter self-interactions require $m_{\tilde{\gamma}} \sim 10\ {\rm GeV} - 10\ {\rm TeV}$, and so a μ-term of the form $\mu \sim (1/16\pi^2) M_{3/2}$, while parametrically incorrect, will yield phenomenologically viable numerical values for μ. There are several proposed mechanisms for generating μ-terms in the visible sector of AMSB models; see, for example, Refs. [18–20]. In these mechanisms, the form of μ is typically $f(\lambda_i)/(16\pi^2) M_{3/2}$, where $f(\lambda_i)$ is a function of new Yukawa couplings. For $f(\lambda_i) \sim 1$, these mechanisms solve the μ problem in the MSSM, and similar mechanisms in the hidden sector would provide numerically correct μ-terms for this model of WIMPless dark matter. It would be more satisfying, however, to find μ-term mechanisms that provide the parametrically correct form $\mu \sim (g^2/16\pi^2) M_{3/2}$. This is beyond the scope of this work, but we note that, in contrast to the traditional μ problem of the visible sector, which requires both $\mu \sim m_{\rm weak}$ and $\sqrt{B} \sim m_{\rm weak}$, in the hidden sector, the constraints on B are less stringent, which may open new avenues for μ-term generation.

Finally, we note that we have made several assumptions in the interest of simplicity. More general models with non-universal charges q_i, non-universal μ-terms, or non-vanishing B-terms may have interesting features. In addition, we have assumed that there are no interactions between the visible and hidden sector, which leaves the AMSB collider phenomenology untouched and eliminates direct and indirect dark matter signals. One could introduce connector particles with both visible and hidden sector charges to induce such signals. A special motivation for introducing such interactions is that, as shown in Sec. V, this framework provides the possibility of dark matter particles with a naturally correct thermal relic density, but masses ~ 10 GeV, that is, at the scale indicated by current direct detection anomalies. Such connector particles could allow the lightest visible sector model to decay to the hidden sector, providing collider signals of the hidden sector, and would also induce mixing between the hidden and visible photons, with a host of possible implications.

Acknowledgments

We thank Manoj Kaplinghat, Yuri Shirman, and especially Yael Shadmi for many helpful conversations. The work of JLF was supported in part by NSF grants PHY–0653656 and PHY–0970173. The work of VR was supported in part by DOE grant DE-FG02-04ER-41298. The work of ZS was supported in part by DOE grant FG-03-94ER40837.

---

[1] J. L. Feng and J. Kumar, "The WIMPless Miracle: Dark-Matter Particles without Weak-Scale Masses or Weak Interactions," {\emPhys.Rev.Lett.}{\bf101}(2008)231301, {\ttarXiv:0803.4196[hep-ph]}.

[2] J. L. Feng, H. Tu, and H.-B. Yu, "Thermal Relics in Hidden Sectors," {\emJCAP}{\bf0810}(2008)043, {\ttarXiv:0808.2318[hep-ph]}.

[3] J. L. Feng, J. Kumar, and L. E. Strigari, "Explaining the DAMA Signal with WIMPless Dark Matter," {\emPhys.Lett.}{\bfB670}(2008)37--40, {\ttarXiv:0806.3746[hep-ph]}.

[4] J. L. Feng, J. Kumar, J. Learned, and L. E. Strigari, "Testing the Dark Matter Interpretation of the DAMA/LIBRA Result with Super-Kamiokande,"

{\emJCAP}{\bf0901}(2009)032, {\ttarXiv:0808.4151[hep-ph]}.

[5] J. Kumar, J. G. Learned, and S. Smith, "Light Dark Matter Detection Prospects at Neutrino Experiments," {\emPhys.Rev.}{\bfD80}(2009)113002, {\ttarXiv:0908.1768[hep-ph]}.

[6] V. Barger, J. Kumar, D. Marfatia, and E. M. Sessolo, "Fermion WIMPless Dark Matter at DeepCore and IceCube," {\emPhys.Rev.}{\bfD81}(2010)115010, {\ttarXiv:1004.4573[hep-ph]}.

[7] G. Zhu, "WIMPless dark matter and the excess gamma rays from the Galactic center," {\emPhys.Rev.}{\bfD83}(2011)076011, {\ttarXiv:1101.4387[hep-ph]}.

[8] D. McKeen, "WIMPless Dark Matter and Meson Decays with Missing Energy," {\emPhys.Rev.}{\bfD79}(2009)114001, {\ttarXiv:0903.4982[hep-ph]}.

[9] G. K. Yeghiyan, "Υ Decays into Light Scalar Dark Matter," {\emPhys.Rev.}{\bfD80}(2009)115019, {\ttarXiv:0909.4919[hep-ph]}.

[10] D. McKeen, "Contributions to the Muon's Anomalous Magnetic Moment from a Hidden Sector," {\emAnnalsPhys.}{\bf326}(2011)1501--1514, {\ttarXiv:0912.1076[hep-ph]}.

[11] A. Badin and A. A. Petrov, "Searching for light Dark Matter in heavy meson decays," {\emPhys.Rev.}{\bfD82}(2010)034005, {\ttarXiv:1005.1277[hep-ph]}.

[12] J. Alwall, J. L. Feng, J. Kumar, and S. Su, "Dark Matter-Motivated Searches for Exotic 4th Generation Quarks in Tevatron and Early LHC Data," {\emPhys.Rev.}{\bfD81}(2010)114027, {\ttarXiv:1002.3366[hep-ph]}.

[13] J. Goodman *et al.*, "Constraints on Dark Matter from Colliders," {\emPhys.Rev.}{\bfD82}(2010)116010, {\ttarXiv:1008.1783[hep-ph]}.

[14] J. Alwall, J. L. Feng, J. Kumar, and S. Su, "B's with Direct Decays: Tevatron and LHC Discovery Prospects in the $b\bar{b}$+MET Channel," {\ttarXiv:1107.2919[hep-ph]}.

[15] L. Randall and R. Sundrum, "Out of this world supersymmetry breaking," {\emNucl.Phys.}{\bfB557}(1999)79--118, {\ttarXiv:hep-th/9810155}.

[16] G. F. Giudice, M. A. Luty, H. Murayama, and R. Rattazzi, "Gaugino Mass without Singlets," *JHEP* **12** (1998) 027, {\ttarXiv:hep-ph/9810442}.

[17] M. Luty and R. Sundrum, "Anomaly mediated supersymmetry breaking in four dimensions, naturally," {\emPhys.Rev.}{\bfD67}(2003)045007, {\ttarXiv:hep-th/0111231}.

[18] A. Pomarol and R. Rattazzi, "Sparticle masses from the superconformal anomaly," *JHEP* **05** (1999) 013, {\ttarXiv:hep-ph/9903448}.

[19] Z. Chacko, M. A. Luty, I. Maksymyk, and E. Ponton, "Realistic anomaly-mediated supersymmetry breaking," *JHEP* **04** (2000) 001, {\ttarXiv:hep-ph/9905390}.

[20] E. Katz, Y. Shadmi, and Y. Shirman, "Heavy thresholds, slepton masses and the mu term in anomaly mediated supersymmetry breaking," *JHEP* **08** (1999) 015, {\ttarXiv:hep-ph/9906296}.

[21] J. L. Feng and Y. Shadmi, "WIMPless Dark Matter from Non-Abelian Hidden Sectors with Anomaly-Mediated Supersymmetry Breaking," {\emPhys.Rev.}{\bfD83}(2011)095011, {\ttarXiv:1102.0282[hep-ph]}.

[22] S. Das and K. Sigurdson, "Cosmological Limits on Hidden Sector Dark Matter," {\ttarXiv:1012.4458[astro-ph.CO]}.

[23] J. L. Feng, M. Kaplinghat, H. Tu, and H.-B. Yu, "Hidden Charged Dark Matter," {\emJCAP}{\bf0907}(2009)004, {\ttarXiv:0905.3039[hep-ph]}.

[24] J. L. Feng, J.-F. Grivaz, and J. Nachtman, "Searches for Supersymmetry at High-Energy Colliders," {\emRev.Mod.Phys.}{\bf82}(2010)699--727, {\ttarXiv:0903.0046[hep-ex]}.

[25] **ATLAS and CMS** Collaboration, H. Bachacou, "Beyond the Standard Model at the LHC,". talk given at the XXV International Symposium on Lepton Photon Interactions at High Energies (Lepton Photon 11).

[26] H. M. Hodges, "Mirror baryons as the dark matter," {\emPhys.Rev.}{\bfD47}(1993)456--459.

[27] Z. G. Berezhiani, A. D. Dolgov, and R. N. Mohapatra, "Asymmetric Inflationary Reheating and the Nature of Mirror Universe," {\emPhys.Lett.}{\bfB375}(1996)26--36, {\ttarXiv:hep-ph/9511221}.

[28] G. Mangano *et al.*, "Relic neutrino decoupling including flavour oscillations," {\emNucl.Phys.}{\bfB729}(2005)221--234, {\ttarXiv:hep-ph/0506164}.

[29] R. H. Cyburt, B. D. Fields, K. A. Olive, and E. Skillman, "New BBN limits on Physics Beyond the Standard Model from He4," {\emAstropart.Phys.}{\bf23}(2005)313--323, {\ttarXiv:astro-ph/0408033}.

[30] B. Fields and S. Sarkar, "Big-bang nucleosynthesis (PDG mini-review)," {\ttarXiv:astro-ph/0601514}.

[31] **WMAP** Collaboration, E. Komatsu *et al.*, "Seven-Year Wilkinson Microwave Anisotropy

Probe (WMAP) Observations: Cosmological Interpretation," {\emAstrophys.J.Suppl.}{\bf192}(2011)18, {\ttarXiv:1001.4538[astro-ph.CO]}.

[32] J. Hamann, J. Lesgourgues, and G. Mangano, "Using BBN in cosmological parameter extraction from CMB: A Forecast for PLANCK," {\emJCAP}{\bf0803}(2008)004, {\ttarXiv:0712.2826[astro-ph]}.

[33] K. Ichikawa, T. Sekiguchi, and T. Takahashi, "Probing the Effective Number of Neutrino Species with Cosmic Microwave Background," {\emPhys.Rev.}{\bfD78}(2008)083526, {\ttarXiv:0803.0889[astro-ph]}.

[34] L. Colombo, E. Pierpaoli, and J. Pritchard, "Cosmological parameters after WMAP5: forecasts for Planck and future galaxy surveys," {\emMon.Not.Roy.Astron.Soc.}{\bf398}(2009)1621, {\ttarXiv:0811.2622[astro-ph]}.

[35] S. Joudaki and M. Kaplinghat, "Dark Energy and Neutrino Masses from Future Measurements of the Expansion History and Growth of Structure," {\ttarXiv:1106.0299[astro-ph.CO]}.

[36] L. Ackerman, M. R. Buckley, S. M. Carroll, and M. Kamionkowski, "Dark Matter and Dark Radiation," {\emPhys.Rev.}{\bfD79}(2009)023519, {\ttarXiv:0810.5126[hep-ph]}.

[37] J. Miralda-Escudé, ``{ATestoftheCollisionalDarkMatterHypothesisfromClusterLensing},''{\em\ apj}{\bf564}(Jan.,2002)60--64, {\ttarXiv:astro-ph/0002050}.

[38] D. A. Buote, T. E. Jeltema, C. R. Canizares, and G. P. Garmire, "Chandra Evidence for a Flattened, Triaxial Dark Matter Halo in the Elliptical Galaxy NGC 720," {\emAstrophys.J.}{\bf577}(2002)183--196, {\ttarXiv:astro-ph/0205469}.

[39] P. J. Humphrey *et al.*, "A Chandra View of Dark Matter in Early-Type Galaxies," {\emAstrophys.J.}{\bf646}(2006)899--918, {\ttarXiv:astro-ph/0601301}.

[40] **DAMA** Collaboration, R. Bernabei *et al.*, "First results from DAMA/LIBRA and the combined results with DAMA/NaI," {\emEur.Phys.J.}{\bfC56}(2008)333--355, {\ttarXiv:0804.2741[astro-ph]}.

[41] R. Bernabei *et al.*, "New results from DAMA/LIBRA," {\emEur.Phys.J.}{\bfC67}(2010)39--49, {\ttarXiv:1002.1028[astro-ph.GA]}.

[42] **CoGeNT** Collaboration, C. E. Aalseth *et al.*, "Results from a Search for Light-Mass Dark

Matter with a P- type Point Contact Germanium Detector,"
{\emPhys.Rev.Lett.}{\bf106}(2011)131301, {\ttarXiv:1002.4703[astro-ph.CO]}.

[43] C. E. Aalseth *et al.*, "Search for an Annual Modulation in a P-type Point Contact Germanium Dark Matter Detector," {\ttarXiv:1106.0650[astro-ph.CO]}.